FLOW BOILING HEAT TRANSFER COEFFICIENT OF DI-WATER/SiO_2 (15 NM AND 80 NM) NANOFLUIDS INSIDE MICROCHANNELS

Tiago Augusto Moreira, Thermal and Fluids, tiago.moreira@usp.br
Francisco Júlio do Nascimento, Thermal and Fluids, f.nascimento@gmail.com
Gherhardt Ribatski, Thermal and Fluids, ribatski@sc.usp.br

Abstract. *The present paper reports experimental results for the heat transfer coefficient during flow boiling of DI-water and DI-water/SiO_2 nanofluids. The experiments were performed inside a 1.1 mm ID and 200 mm long stainless steel (AISI-304) tube. Nanofluids were prepared for two sizes of SiO_2 nanoparticles, 15 nm and 80 nm, and three volumetric concentrations, 0.001, 0.01 and 0.1%. Flow boiling results were also obtained for DI-water on the surfaces coated with nanoparticles. The coatings were performed through flow boiling of nanofluids prior the tests with DI-water. For the nanofluid composed of DI-water/SiO_2 (15 nm) nanofluid, the experimental data showed a reduction of the heat transfer coefficient for volumetric concentrations of 0.1 and 0.001%. Variations in the heat transfer coefficient within the uncertainty range of their measurements were noted for volumetric concentrations of the 0.01%. Results for DI-water/SiO_2 (80 nm) presented variations of the heat transfer coefficient within the uncertainty range of their measurements except for the highest mass velocity, for which the heat transfer coefficient for volumetric concentrations of 0.01 and 0.001% was higher than for flow boiling of DI-water in a clean tube. The DI-water results on the surfaces coated with nanoparticles showed a reduction of the heat transfer coefficient for the surface coated with SiO_2 (15 nm) and no significant variations for the surface coated with 80 nm nanoparticles. Based on these results, it was concluded that the modification of the surface texture due to the deposition of nanoparticles affects the heat transfer coefficient behavior.*

Keywords*: heat transfer coefficient, flow boiling, nanofluids, microchannels*

1. NOMENCLATURE

ABN – Surface coated with nanofluids
BBN – Surface without deposition
ID – Internal diameter
G – Mass velocity, kg/m^2s
h – Heat transfer coefficient, $W/m^2°C$
q – Heat flux, W/m^2
T_{wall} – Temperature of the internal tube wall, °C
T_{bulk} – Fluid bulk temperature, °C
ω - Volumetric concentration, %

1. INTRODUCTION

Great effort has been demanded to understand the complex mechanisms involved during heat transfer processes of nanofluids since the pioneer work of Choi and Eastman (1995). In their study, nanoparticles were added to a fluid in order to enhance its thermal conductivity. Besides altering the transport properties of the base fluid, the boiling process of nanofluids on a heated surface leads to deposition of nanoparticles on the boiled surface, affecting the boiling mechanism. Controversial conclusions are found in the literature about the effect of nanofluids on the heat transfer coefficient during boiling processes. On the other hand, it is a fact that the critical heat flux increases with adding nanoparticles to a base fluid. Some literature reviews concerning experimental investigations of the boiling phenomena of nanofluids are listed below and are suggested to those interested on the state of the art concerning this topic: Eastman et al. (2004), Das et al. (2006), Cheng et al. (2008), Wang and Mujumdar (2008), Yu et al. (2008), Taylor and Phelan (2009), Wen et al. (2009), Godson et al. (2010), Barber et al. (2011), Cheng and Liu (2013), Taylor et al. (2013), Wu and Zhao (2013), Vafaei and Borca-Tasciuc (2014).

From an analyses of the literature reviews above mentioned, it is concluded that flow boiling of nanofluids inside narrow channels was rarely investigated. Compared to results for the heat transfer coefficient during flow boiling of pure water, Wu et al. (2009) found increments up to 20% for convective boiling of alumina-water nanofluids. Boudouh et al. (2010) found increments of more than 100% in the heat transfer coefficient for flow boiling of copper-water nanofluids. Chehade et al. (2013), using silver-water nanofluids, found average increments for the flow boiling heat transfer coefficient up to 136% compared to pure water. Despite of the HTC enhancement pointed out by these

studies, additional investigations are still needed in order to characterize the effect of nanofluids on the flow boiling mechanism inside microchannels.

In the present study, an investigation about the effect of nanoparticle dimension on the heat transfer coefficient of DI-water/SiO_2 nanofluids inside a stainless steel (AISI-304) 1.1 mm ID tube is performed. Two sizes of SiO_2 spherical nanoparticles were used in the experimental campaign 15 nm and 80 nm. Experiments for DI-water on the surface coated with nanoparticles were also performed in order to evaluate the effect of the size of the deposited nanoparticle dimension on the heat transfer coefficient behavior.

2. EXPERIMENTAL APPARATUS AND PROCEDURE

2.1. Experimental facility

Figure 1 illustrates the experimental apparatus and details of the test section. In the facility, the test fluid is driven from the reservoir through the circuit by a gear pump (Micropump GA-T23). The mass flow rate is estimated from single-phase pressure drop measurements through a 2.0 mm ID, 100 mm long quartz tube using a differential pressure transducer (Endress+Hauser PMD75) with a measurement span of 0-3 kPa. Calibration curves were previously adjusted correlating the pressure drop and mass flow rate using as reference the mass deposition in a digital analytical balance (precision 0.01 g). During these testes, the test facility was run as an open circuit. Such procedure was implemented to avoid possible effects on the flow rate measurements of nanoparticles deposition on the internal parts of commercial and non-internally inspectable flow meters. The error associated with the mass flow meter was found equal to 4.6% of the measured value with reliability of 95.4%.

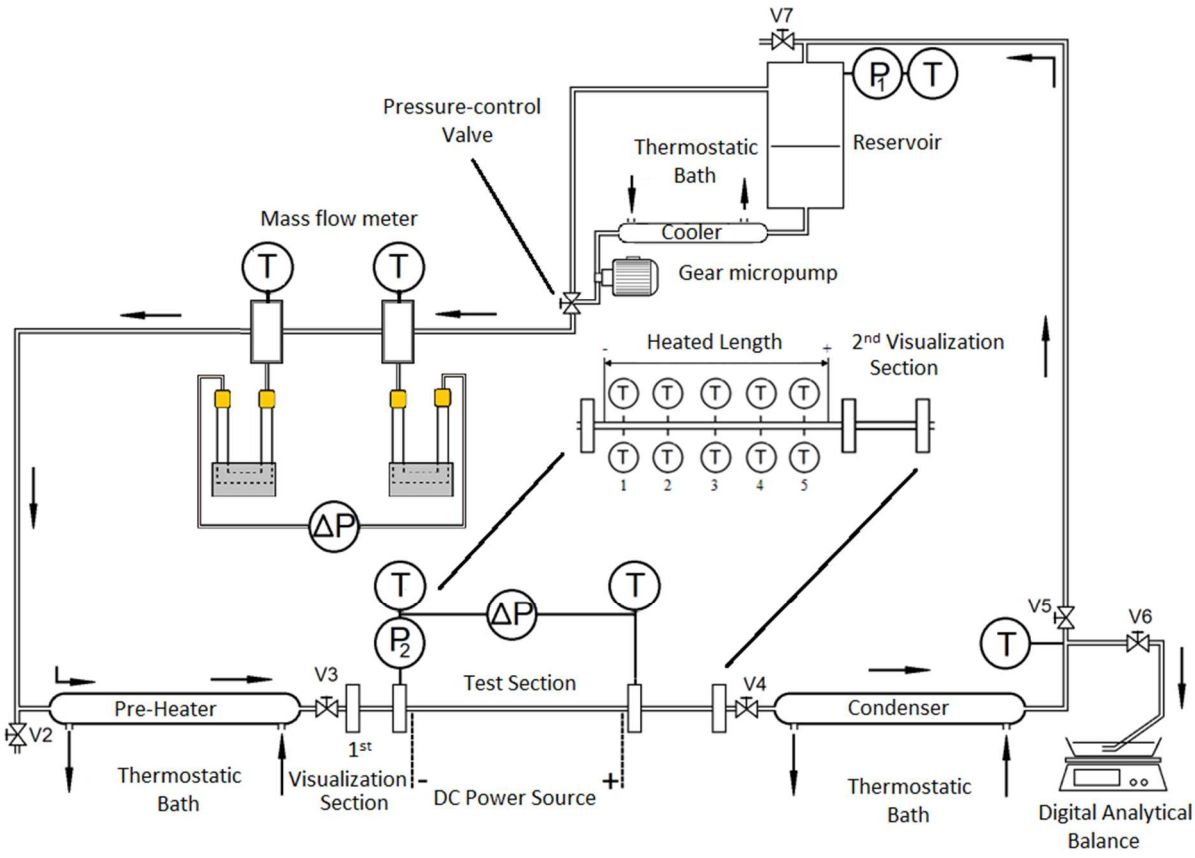

Figure 1. Illustration of the test facility.

A pre-heater consisting of a tube-in-tube heat exchanger is used to impose the inlet temperature of the test fluid at the test section. This heat exchanger uses as heating source a thermal fluid (capable of working at temperatures up to

317°C) whose temperature is controlled by a thermal bath. Needle valves located upstream and downstream of the test section are used to minimize two-phase flow oscillations due to the confined bubble formation. At the test section entrance, measurements of bulk temperature, using a thermocouple positioned within the flow, and absolute pressure, using a pressure transducer (Endress+Hauser PMP131 for 0-400 kPa) were performed. The differential pressure along the test section was measured with a differential pressure transducer (Endress+Hauser PMD75 for 0-300 kPa). The outlet temperature was measured through a thermocouple positioned within the flow. The wall temperature was measured with thermocouples fixed on the external wall of the test section at the top and bottom of each section. Wall temperatures were measured at 5 cross-sections distributed along the heated length of the test tube.

The test section is a stainless steel tube (AISI-304) with internal diameter of 1.1 mm and 200 mm long. The heating effect of the test section was obtained by supplying electrical current from a DC power source (TDK-Lambda GEN 20V-76A) directly to the test surface. All temperatures were measured with K-type thermocouples with hot junction diameters of 0.152 mm. Just downstream the test section is a 1.0 mm ID and 100 mm long quarts tube, installed in order to allow two-phase flow visualizations with a high-speed camera. Downstream the transparent tube is a heat exchanger (condenser) responsible for condensing and subcool the test fluid by rejecting heat to a secondary fluid which temperature is controlled by a second thermal bath. The condenser, the pre-heater, the flow meter and the reservoir are made of borosilicate glass, allowing the evaluation of deposition of nanoparticles along the circuit. To record the data and to monitor and control the experimental apparatus, a LabView program was used with a National Instruments data acquisition system (SCXI-1000 with SCXI-1102 thermocouples module).

The test facility and the data regression procedure were validated through comparisons of heat transfer and pressure drop experimental results for single-phase flow and well-established predictive methods from literature (see Moreira et al., 2015).

2.2. Experimental procedures

Experimental campaign and analysis:

Heat transfer coefficient results were obtained for: (i) DI-water on the surface as received from the manufacturer (BBN); (ii) DI-water/SiO_2 (80 nm) and DI-water/SiO_2 (15 nm) nanofluids; and (iii) DI-water on the surface after boiling the nanofluids (ABN). Two different test tubes were utilized, one for each nanofluid tested. The experiments for each tube were performed always according to the following chronological order: DI-water BBN – nanofluid – DI-water ABN. A summary of the experimental conditions are displayed in Tab. 1.

Table 1. Experimental conditions.

Fluid	Mass velocity (kg/m^2s)	Heat flux (kW/m^2)	Volumetric concentration (%)
DI-water (BBN)	600/400/200	100-350	0.001/0.01/0.1
DI-water/SiO_2 (80 nm)	600/400/200	100-350	0.001/0.01/0.1
DI-water/SiO_2 (15 nm)	600/400/200	100-350	0.001/0.01/0.1
DI-water (ABN)	600/400/200	100-350	0.001/0.01/0.1

Before been charged in the circuit, the test fluid was boiled for a period of 30 minutes in order of eliminating non-condensable gases. The experimental circuit was firstly evacuated down to an absolute pressure of 10 kPa, and then charged with DI-water. The tests were performed for a saturation temperature at the test section outlet of 102 ± 3°C, subcooling at the test section inlet of 25°C and vapor quality at the test section outlet ranging from 0.01 to 0.5.

The local heat transfer coefficient, h, was estimated according to the Newton's cooling law, as follows:

$$h = \frac{q}{(T_{wall} - T_{bulk})} \tag{1}$$

The temperature at each one of the five cross-sections with thermocouples was estimated by averaging the measurements at the top and bottom of the tube external surface. Based on this value for each cross section, the wall

temperature of the inner surface, T_{wall}, was estimated by solving the heat diffusion equation assuming one-dimensional heat conduction through the wall, uniform heat generation by joule effect and adiabatic external surface. To estimate the fluid bulk temperature, T_{bulk}, firstly, based on the heat flux and the measured temperature and pressure at the test section inlet, the subcooled region length, the single-phase pressure drop over its length, and the saturation temperature at the beginning of the saturated region were calculated by solving simultaneously an equation of state relating saturation temperature and pressure plus single-phase pressure drop and a local energy balance. The overall pressure drop over the saturated region was then determined by subtracting the single-phase pressure drop from the measured total pressure drop. After that, a constant pressure drop gradient, given as the ratio of the overall pressure drop over the saturated region and the corresponding length, was assumed from the beginning of the saturated region until the end of the test section. Then, the saturation temperature was calculated from the estimated local pressure. The heat flux, q, was calculated as the ratio between the electrical power supplied to the test section and its internal area based on the heated length. The electrical power was calculated as the product between the electrical current and the voltage supplied by the DC power source. The local vapor quality was estimated based on determined by an energy balances over the corresponding heated lengths.

Temperature measurements were calibrated and the temperature uncertainty was evaluated according to the procedure suggested by Abernethy and Thompson (1973). Accounting for all instrument errors, uncertainties for the calculated parameter were estimated using the method of sequential perturbation according to Taylor and Kuyatt (1994). The experimental heat transfer coefficient error was always lower than 20%. The heat transfer coefficient average error was 10.6%.

Nanofluids manufacturing

The nanofluids were prepared according to the two-steps method, which consists of adding SiO_2 nanoparticles (with 80 nm or 15 nm diameter), weighed through a digital analytical balance (resolution of 1 µg), to a base fluid (DI-water) and dispersing them through ultrasonication during a period of 30 minutes (Coleparmer CP505).

3. RESULTS

Figure 2 illustrates the heat transfer coefficient behavior with varying vapor quality for DI-water/SiO_2 nanofluids, DI-water BBN and ABN. According to this figure, distinct behaviors were obtained with varying the nanoparticle dimension. Generally, the heat transfer coefficient presents a reduction for the DI-water/SiO_2 (15 nm) nanofluid and variations within the uncertainty range of its measurements for the DI-water/SiO_2 (80 nm), both in relation to the DI-water BBN. Moreover, the comparison between results for the DI-water BBN and ABN indicates a reduction of the heat transfer coefficient for the surface coated with SiO_2 (15 nm) nanoparticles and no significant variations for the surface covered by SiO_2 (80 nm).

SiO_2 (15 nm) nanofluid and covered surface

For the volumetric concentrations of 0.01%, independently of the mass velocity, and 0.001% for G=200 kg/m^{2}s, the heat transfer coefficient varies within the uncertainty of its measurements compared to the results for DI-water BBN. The heat transfer coefficient for the volumetric concentration of 0.1% is lower than the values obtained for the DI-water BBN. It is worth to highlight that for experimental conditions characterized by ω=0.1%, x>0.13 and G=200 and 400 kg/m^{2}s, the heat transfer coefficient is less than half of the values obtained for DI-water BBN. Under low vapor quality conditions and G=200 kg/m^{2}s, the results for the heat transfer coefficient of DI-water BBN and nanofluids with volumetric concentrations of 0.01 and 0.001 are almost similar.

For DI-water BBN and nanofluids with volumetric concentrations of 0.01 and 0.001, it is noted that the heat transfer coefficient decreases with increasing vapor quality under conditions of low vapor quality and G=200 kg/m^{2}s. This behavior is observed until a vapor quality for which the heat transfer coefficient presents a minimum value. Then, further increases in the vapor quality implies on increasing the heat transfer. For DI-water ABN, BBN and nanofluids and mass velocities of 600 and 400 kg/m^{2}s, variations of the heat transfer coefficient with increasing vapor quality were within the uncertainty range of their measurements, indicating a predominance of nucleate boiling effects.

For flow boiling of DI-water on the surface coated with SiO_2 (15 nm) nanoparticles (DI-water ABN) a reduction of the heat transfer coefficient in comparison to DI-water BBN is observed in Fig. 2. The present authors speculate that the layer formed on the surface due to the deposition of nanoparticles presents less cavities with the size within the range necessary for their activation. This behavior implies on the suppression of the nucleate boiling effects, reducing the heat transfer coefficient. Based on the results for the heat transfer coefficient obtained for the SiO_2 (15 nm)

nanofluids and DI-water ABN in comparison with the DI-water BBN it is concluded that the insertion of the SiO_2 (15 nm) nanoparticles impacts directly on the nucleate boiling, reducing its effects.

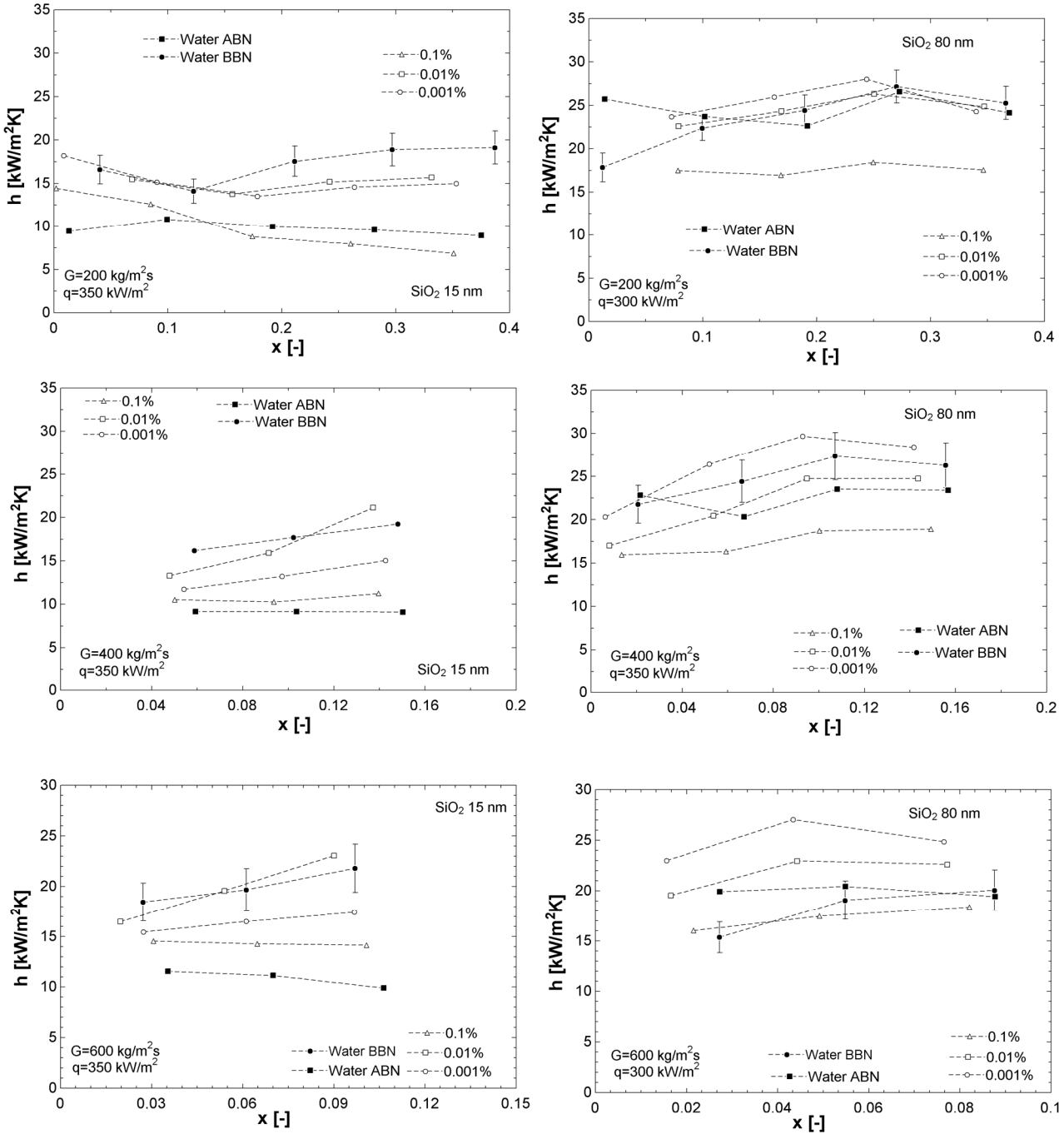

Figure 2. Heat transfer coefficient results for SiO_2 nanofluids, DI-water BBN and DI-water ABN.

<u>SiO_2 (80 nm) nanofluid and covered surface</u>

For mass velocities of 200 and 400 kg/m²s, the differences of the heat transfer coefficient among DI-water BBN, DI-water ABN andDI-water/SiO_2 (80 nm) nanofluids with volumetric concentrations of 0.01 and 0.001% were within the uncertainty range of the heat transfer coefficient measurements. For G=600 kg/m²s and volumetric concentrations of 0.001 and 0.01%, the heat transfer coefficient of the nanofluids are higher than the values obtained for

DI-water BBN. For ω=0.1% and G=200 and 400 kg/m^{2}s a reduction of the heat transfer coefficient was observed compared the results for DI-water BBN. Under the same volumetric concentration (ω=0.1%) and G=600 kg/m^{2}s the differences of the heat transfer coefficient between the nanofluid and DI-water BBN were marginal.

For the DI-water BBN and nanofluids with volumetric concentrations 0.01 and 0.001%, independently of mass velocity, it is noted that the heat transfer coefficient increases with increasing vapor quality. This behavior is typical of flow boiling dominated by convective effects. For ω=0.1% and independently of mass velocity, the effect of the vapor quality on the heat transfer coefficient is only marginal. Such behavior is typical of conditions under predominance of nucleate boiling effects.

The results of the heat transfer coefficient for DI-water ABN under low vapor quality conditions and mass velocities of 200 and 600 kg/m^{2}s are higher than the values obtained for DI-water BBN. This result suggests the enhancement of nucleate boiling effects due to deposition of nanoparticles. For DI-water ABN and G=400kg/m^{2}s, no significant variations on the heat transfer coefficient compared to DI-water BBN were observed.

It is speculated by the present authors that the deposition of SiO_2 (80 nm) nanoparticles on the surface provides an increment of the number of active nucleation cavities. This speculation is in accordance with the experimental trends observed for results for G=600 kg/m^{2}s. For these results, the fact that the heat transfer coefficient for the nanofluids with volumetric concentration of 0.01 and 0.001% is higher than for DI-water BBN is attributed to the enhancement of nucleate boiling effects.

4. CONCLUSIONS

Based on the analyses of the results obtained in the present study, the following conclusions are presented:

i. In general, the addition of SiO_2 (15 nm) according to volumetric concentrations of 0.001 and 0.01% causes a reduction of the heat transfer coefficient compared to DI-water BBN. For nanofluids containing SiO_2 (80 nm) nanoparticles, the variations of the heat transfer coefficient compared to DI-water BBN, are, in majority, within the uncertainty range of the measurements of the heat transfer coefficient. For G=600 kg/m^{2}s and volumetric concentrations of 0.01 and 0.001%, the heat transfer coefficient for the nanofluids containing SiO_2 (80 nm) is higher than for DI-water BBN. A decrease on the heat transfer coefficient for the SiO_2 (80 nm) nanofluids in relation to the DI-water BBN was observed for ω=0.1% and G=400 and 200 kg/m^{2}s.

ii. The DI-water on the surface covered with 15 nm nanoparticles showed a reduction of the heat transfer coefficient in relation to DI-water BBN, as displayed in Fig. 2. For the surface coated with 80 nm nanoparticles, in general, differences of the heat transfer coefficient between DI-water ABN and DI-water BBN were within the uncertainty range of the measurements of the heat transfer coefficient. For G=200 and 600 kg/m^{2}s and under low vapor quality conditions, the heat transfer coefficient for DI-water ABN presented higher values than for DI-water BBN, indicating an increment on the nucleate boiling effects under these conditions.

iii. Finally, based on the results displayed in Fig. 2, it is clear that the nanoparticles affect the heat transfer coefficient during the flow boiling of nanofluids by modifying the surface texture due to deposition. This change on the surface structure provided by the deposition affects the nucleate boiling and consequently, the heat transfer behavior. Moreover, the characteristic of this effect depends on how the nanoparticles fill the cavities on the surface that may either increase or decrease the number of cavities on the active range of bubble nucleation compared to the original surface.

5. REFERENCES

ABERNETHY R.B., THOMPSON J.W., **Handbook uncertainty in gas turbine measurements**, Arnold Engineering Development Center, Arnold Air Force Station, Tennesse, 1973.

BARBER, J., BRUTIN, D., TADRIST, L. A review on boiling heat transfer enhancement with nanofluids. **Nanoscale Research Letters**, v. 6, p. 1-16, 2011.

BOUDOUH, M., GUALOUS, H.L., DE LABACHELERIE, M. Local convective boiling heat transfer and pressure drop of nanofluid in narrow rectangular channels. **Applied Thermal Engineering**, v. 30, p. 2619–2631, 2010.

CHEHADE, A.A., GUALOUS, H.L., LE MASSON, S., FARDOUN, F., BESQ, A. Boiling local heat transfer enhancement in minichannels using nanofluids, **Nanoscale Research Letters**, v. 8, p. 1-20, 2013.

CHENG, L., BANDARRA FILHO, E.P., THOME, J.R. Nanofluid Two-Phase Flow and Thermal Physics: A New Research Frontier of Nanotechnology and Its Challenges. **Journal of Nanoscience and Nanotechnology**, v. 8, p. 3315–3332, 2008.

CHENG, L., LIU, L. Boiling and two-phase flow phenomena of refrigerant-based nanofluids: Fundamentals, applications and challenges. **International Journal of Refrigeration**, v. 36, p. 421–446, 2013.
CHOI, S.U.S., EASTMAN, J.A. Enhancing Thermal Conductivity of Fluids with Nanoparticles. In: Proceedings of **ASME INTERNATIONAL MECHANICAL ENGINEERING CONGRESS & EXPOSITION**. San Francisco, CA, USA, 1995.
DAS, S.K., CHOI, S.U.S., PATEL, H.E. Heat Transfer in Nanofluids - A Review. **Heat Transfer Engineering**, v. 27, p. 3–19,2006
EASTMAN, J. A., PHILLPOT, S.R., CHOI, S.U.S., KEBLINSKI, P.Thermal Transport in Nanofluids. ***Annual Review of Materials Research***, v. 34, p. 219–246, 2004.
GODSON, L., RAJA, B., MOHAN LAL, D., WONGWISES, S. Enhancement of heat transfer using nanofluids - An overview. **Renewable and Sustainable Energy Reviews**, v. 14, p. 629–641, 2010.
MOREIRA, T. A., NASCIMENTO, F. J., RIBATSKI, G. Flow boiling heat transfer coefficient of DI-water/SiO2 nanofluid inside a 1.1 mm round microchannel. In: Proceedings of **ASME INTERNATIONAL CONFERENCE ON NANOCHANNELS, MICROCHANNELS AND MINICHANNELS**, San Francisco, CA, USA, 2015.
TAYLOR, B. N., KUYATT, C. E. Guidelines for evaluating and expressing the uncertainty of NIST measurement results, **National Institute of Standarts and Technology (NIST)**, Technical note 1297, 1994.
TAYLOR, R., COULOMBE, S., OTANICAR, T., PHELAN, P., GUNAWAN, A., LV, W., ROSENGARTEN, G., PRASHER, R., TYAGI, H. Small particles, big impacts: A review of the diverse applications of nanofluids. **Journal of Applied Physics**, v. 113, p. 1-19, 2013.
TAYLOR, R.A., PHELAN, P.E. Pool boiling of nanofluids : Comprehensive review of existing data and limited new data. **International Journal of Heat and Mass Transfer**, v. 52, p. 5339–5347, 2009.
VAFAEI, S., BORCA-TASCIUC, T. Role of nanoparticles on nanofluid boiling phenomenon: Nanoparticle deposition. **Chemical Engineering Research and Design**, v. 92, p.842–856, 2014.
WANG, X., MUJUMDAR, A.S. A review on nanofluids - Part II: Experiments and applications. **Brazilian Journal of Chemical Engineering**, v. 25, p. 631–648, 2008.
WEN, D., LIN, G., VAFAEI, S., ZHANG, K. Review of nanofluids for heat transfer applications. **Particuology**, v. 7, p. 141–150, 2009.
WU, J.M., ZHAO, J. A review of nanofluid heat transfer and critical heat flux enhancement—Research gap to engineering application. **Progress in Nuclear Energy**, v. 66, p. 13–24, 2013.
WU, X., WU, H., CHENG, P. Pressure drop and heat transfer of Al2O3 -H2O nanofluids through silicon microchannels. **Journal of Micromechanics and Microengineering**, v. 19, p. 1-11, 2009.
YU, W., FRANCE, D.M., ROUTBORT, J.L., CHOI, S.U.S. Review and Comparison of Nanofluid Thermal Conductivity and Heat Transfer Enhancements. **Heat Transfer Engineering**, v. 29, p. 432–460, 2008.

6. ACKNOWLEDGEMENTS

The authors gratefully acknowledge the financial support under contract numbers 2011/13119-0 and 131082/2015-9 given by FAPESP (São Paulo Research Foundation, Brazil) and CNPq (National Council of Technological and Scientific Development, Brazil) respectively, and the CAPES (Coordination for the Improvement of Higher Level Personal, Brazil) for the research grant given through the NANOBIOTEC research program. The authors also acknowledge Mr. José Roberto Bogni for the technical support given to this investigation.

7. RESPONSIBILITY NOTICE

The authors are the only responsible for the printed material included in this paper.